

An Open-source Image Analysis Toolbox for Quantitative Retinal Optical Coherence Tomography Angiography

Yalda Amirmoezzi (MSc)^{1,2}, Mohsen Ghofrani-Jahromi (PhD Candidate)³, Hossein Parsaei (PhD)^{1,2*}, Mehrdad Afarid (MD)⁴, Negar Mohsenipoor (MD)⁴

ABSTRACT

Background: Qualitative and quantitative assessment of retinal perfusion using optical coherence tomography angiography (OCTA) has shown to be effective in the treatment and management of various retinal and optic nerve diseases. However, manual analyses of OCTA images to calculate metrics related to Foveal Avascular Zone (FAZ) morphology, and retinal vascular density and morphology are costly, time-consuming, subject to human error, and are exposed to both inter and intra operator variability.

Objective: This study aimed to develop an open-source software framework for quantitative OCTA (QOCTA). Particularly, for analyzing OCTA images and measuring several indices describing microvascular morphology, vessel morphology, and FAZ morphology.

Material and Methods: In this analytical study, we developed a toolbox or QOCTA using image processing algorithms provided in MATLAB. The software automatically determines FAZ and measures several parameters related to both size and shape of FAZ including area, perimeter, Feret's diameter circularity, axial ratio, roundness, and solidity. The microvascular structure is derived from the processed image to estimate the vessel density (VD). To assess the reliability of the software, three independent operators measured the mentioned parameters for the eyes of 21 subjects. The consistency of the values was assessed using the intraclass correlation coefficient (ICC) index.

Results: Excellent consistency was observed between the measurements completed for the superficial layer, ICC >0.9. For the deep layer, good reliability in the measurements was achieved, ICC >0.7.

Conclusion: The developed software is reliable; hence, it can facilitate quantitative OCTA, further statistical comparison in cohort OCTA studies, and can assist with obtaining deeper insights into retinal variations in various populations.

Citation: Amirmoezzi Y, Ghofrani-Jahromi M, Parsaei H, Afarid M, Mohsenipoor N. An Open-source Image Analysis Toolbox for Quantitative Retinal Optical Coherence Tomography Angiography. *J Biomed Phys Eng.* 2024;14(1):31-42. doi: 10.31661/jbpe.v0i0.2106-1349.

Keyword

Optical Coherence Tomography; Optical Imaging; OCTA; Quantitative OCTA; Retina; Retinal Vascular Density; Foveal Avascular Zone; Computer-Assisted Image Processing

Introduction

Optical coherence tomography (OCT) is a non-invasive, high-resolution imaging technique that was developed for cross-sectional imaging in biological systems. Since its invention in the early 1990s, OCT has emerged as an important imaging technique in

¹Department of Medical Physics and Engineering, School of Medicine, Shiraz University of Medical Sciences, Shiraz, Iran

²Shiraz Neuroscience Research Center, Shiraz University of Medical Sciences, Shiraz, Iran

³Turner Institute for Brain and Mental Health, Monash University, Australia

⁴Poostchi Ophthalmology Research Center, Department of Ophthalmology, School of Medicine, Shiraz University of Medical Sciences, Shiraz, Iran

*Corresponding author: Hossein Parsaei
Department of Medical Physics and Engineering, School of Medicine, Shiraz University of Medical Sciences, Shiraz Iran
E-mail: hparsaei@sums.ac.ir

Received: 9 June 2021
Accepted: 7 August 2021

medicine and ophthalmology [1]. It provides morphological images from retinal tissue with magnification orders of 10 micrometers, which is higher than those of the images provided by magnetic resonance imaging and ultrasonic imaging [2]. OCT provides high-resolution cross-sectional images that are appropriate for evaluating structural changes in various retinal diseases; however, such images cannot be used to assess vascular changes.

To visualize ocular vasculature, several methods such as fluorescein angiography and indocyanine green angiography were developed. Specifically, many functional extensions of OCT were presented [3]. The most recent development is OCT angiography (OCTA) that provides both structural and functional information of the retina and choroid. Moreover, this new imaging technique provides three-dimensional (3D) angiograms of the retinal and choroidal vascular networks [4]. OCTA has shown to be a beneficial modality for evaluating a wide variety of retinal and optic nerve diseases such as age-related macular degeneration (AMD), diabetic retinopathy (DR), artery and vein occlusions, glaucoma, and multiple sclerosis [3].

Several metrics were proposed for quantification of OCTA and ultimately for objective evaluation of retinal and optic nerve diseases, including flow index, vessel density, nonperfusion area measurements, and the shape and size of the foveal avascular zone (FAZ) [5-12]. Initial investigations showed promising results on the repeatability, reproducibility, and discriminability of these indices [7,10]. Previous studies indicated that the area of FAZ in the deep and superficial plexus layer is significantly larger for diabetic eyes [11]. Freiberg et al. reported that the vertical and horizontal diameters of FAZ are significantly different in superficial and deep layers between the healthy and diabetic retinopathy groups [8]. However, manually delineating FAZ is time-consuming and, more importantly, is error-prone due to the presence of numerous artifacts that may

affect image interpretation. Thus, there is a need for algorithms or software packages that can assist in improving the quantitative and qualitative interpretation of OCTA.

This paper presents an interactive software developed in MATLAB for quantitative analysis of OCTA images; the codes are available on GitHub [13]. Particularly, the software provides quantitative measures of vascular density in the region of interest (ROI). The toolbox can be used to calculate several well-known metrics related to size and shape FAZ, including area, form factor, roundness, extent, border irregularity, and convexity. Such quantities may be recorded in longitudinal cohort studies to develop prognosis protocols [14,15]. The remaining sections of the paper describe the images used in the present study, image processing algorithms incorporated in the software, the quantities which can be calculated by the software, and the steps for acquiring these quantities.

Material and Methods

This analytical study was objected to develop a software for quantitative analysis of OCTA images (i.e., QOCTA). The framework of the developed software consists of three fundamental components: 1) an interface to load the image to be analyzed and to crop the desired portion of the image for selecting superficial or deep slices, 2) algorithms for processing the image, segmenting FAZ and calculating vascular density and FAZ metrics, 3) an interface for assessing and manually editing the results (if needed). Figure 1 shows a schematic view of the processing steps involved in the software. The technical aspects of each stage are described below.

Cropping

An OCT image typically contains both superficial and deep acquisitions of retinal vessels. Therefore, the initial step of the analysis is selecting the image corresponding to the desired layer. The region of interest can be

selected either automatically or manually. In the latter, the operator selects the region via the user interface provided in the software. An example is shown in Figure 2.

Preprocessing

Preprocessing was to highlight microvascular structures in the image by improving

the signal-to-noise ratio and reducing motion artifacts and background noise. Here, morphological transformations were used for this purpose. Detailed descriptions of the morphological transformations can be found in [16].

Fundamentally, morphological filtering consists of three steps:

- 1) choosing a structuring element which is

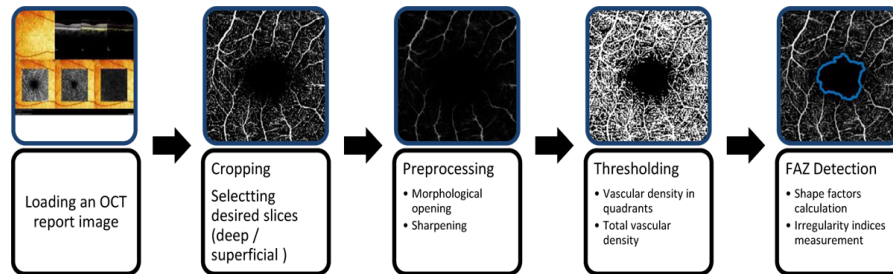


Figure 1: The system flow-chart for estimating the vascular density and Foveal Avascular Zone (FAZ) shape indices.

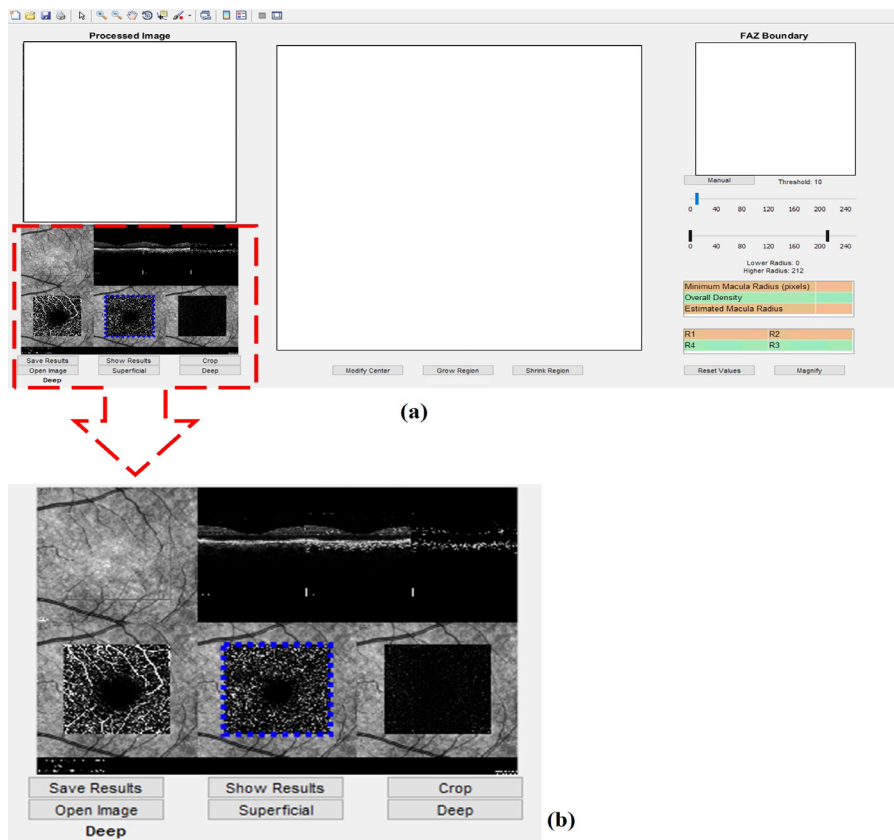


Figure 2: Cropping and selecting the desired image to be analyzed. **a)** In the left column, the box presents the image loaded in the software for analysis. **b)** The user can select one of the images in the square box which belong to the superficial and deep layers of the retina.

a matrix of a specific size with binary values,

2) successively sliding the structuring element pixel by pixel on the original image,

3) applying a non-linear operation each time to yield an output image.

In our algorithm, we employed a flat structuring element to apply the opening operation. This process is repeated multiple times using

flat linear structuring elements of the same length varying angles from 1 to 180 degrees [16]. Consequently, images are sharpened using an algorithm called unsharp masking in which the image is passed through a blurring filter and the resulting image is subtracted from the original one. Figure 3 shows an example of the effectiveness of preprocessing. As shown,

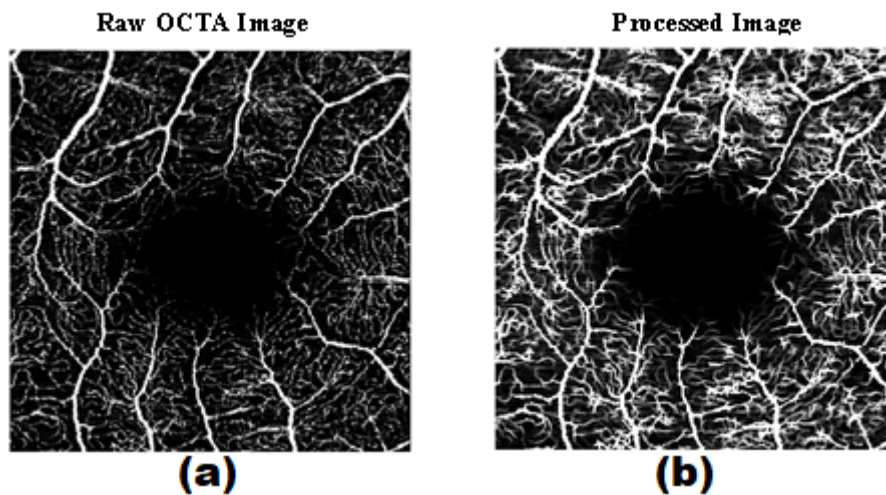


Figure 3: The effectiveness of preprocessing in highlighting microvascular. **a)** Raw image before being processed. **b)** after processing. Vascular structures are more distinguishable in the processed image.

vascular structures are more distinguishable in the processed image.

Vascular Density Estimation

Vessel density is defined as the percentage area occupied by the blood vessels and microvasculature and calculated by first detecting vessels and then calculating the part of the region occupied by the vessels.

To separate microvascular structure from redundant image information (background), we used the “image segmentation” technique. Particularly, a thresholding-based segmentation procedure was used by which each pixel of the given image was classified as “vessel” or “background” by comparing its intensity to a predetermined value. Figure 4 shows the result of applying a threshold on the pre-processed image. As shown, vessels were

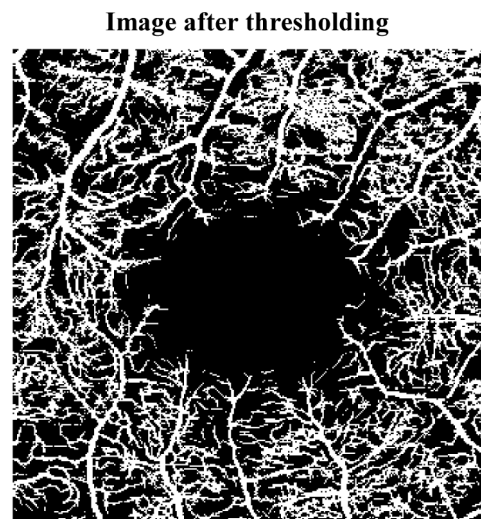


Figure 4: Black and white (binary) retinal optical coherence tomography angiography (OCTA) image after thresholding.

highlighted in the image and separated from background contents.

The value of the threshold can be set manually or can be determined automatically or experimentally. Here, the threshold was set adaptively using the information provided by the image under analysis. Particularly, it was set as the K times of the maximum intensity in the image. The value of parameter K was set to 0.04, determined experimentally. Nevertheless, using the interactive option implemented in the software, the ophthalmologist can compare the segmented and original images and modify the threshold manually to obtain the desired result.

Once the vessels and capillaries are identified in the image, vessel density is calculated as the ratio of pixels associated with them to the total number of pixels in the corresponding ROI. Vascular densities in the four quarters of a rectangular and parafoveal regions set by the user are calculated. Densities may also be computed by specifying the inner and outer radii of the ring around the fovea.

Foveal avascular zone Quantification

Representing FAZ shapes with measurable indices provides the possibility of quantitatively comparing their inter- and intra-group variabilities irrespective of the shape size. In this work, we presented software to calculate

several well-known parameters related to both size and shape of FAZ such as form factor, roundness, extent, convexity, border irregularity, and frequency domain Irregularity [17-20]. Manually measuring these indices particularly delineating FAZ is time-consuming and, more importantly, is error-prone due to the presence of numerous artifacts that may affect image interpretation.

Quantification of FAZ was completed by first identifying FAZ and then calculating several metrics regarding this area. FAZ was obtained via an image segmentation algorithm [21]. Specifically, we used an active contour segmentation algorithm that primarily receives an initial deformable contour. Afterward, the algorithm gradually shapes the curvature according to a set of constraints which is generally obtained from the intensity values of the pixels in the image neighboring the contour. The contour of FAZ can also be manually edited by the user to correct possible segmentation errors. As seen in Figure 5, an expert was re-determined part of the region of the FAZ which was not detected by the algorithm. Figure 6 shows an overview of the software panel and its details.

After segmenting FAZ in a given image, “*regionprops*” function in MATLAB was used to measure FAZ area which is the number of pixels in the region. The following metrics were calculated for the identified FAZ.

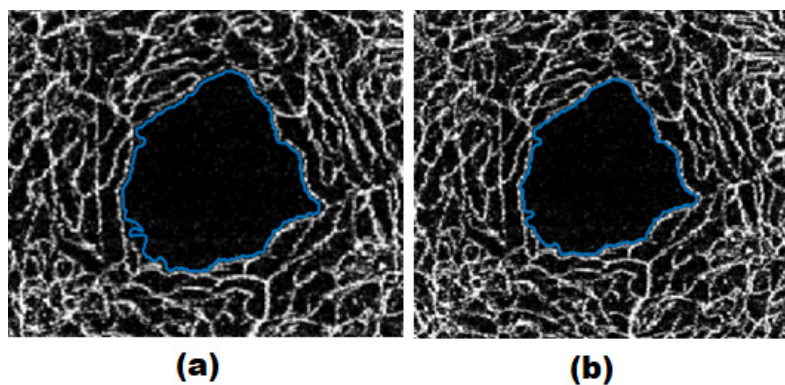


Figure 5: a) Foveal Avascular Zone (FAZ) boundary identified by the software automatically b) FAZ boundary edited by the expert.

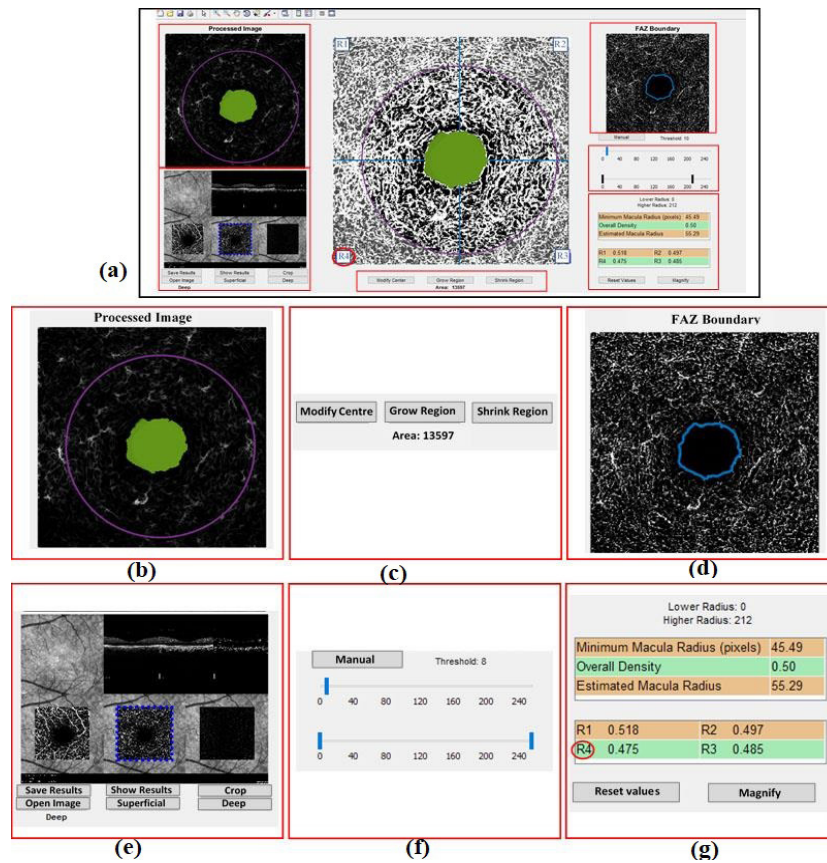


Figure 6: a) Overview of the software panel. b) Showing processed image. c) Buttons for modifying Foveal Avascular Zone (FAZ) such as relocating the center, growing or shrinking FAZ. d) Showing FAZ boundary after post-processing. e) Cropping the desired partition of the image to select deep or superficial slices. f) Options to manually change the threshold value and the inner and outer radii. g) Estimating vascular density in four regions.

Form factor: The relation between the area and perimeter of a shape is represented by the form factor.

$$form\ factor = \frac{4\pi \times area}{(perimeter)^2} \quad (1)$$

Roundness: The similarity of a shape to a circle is evaluated by roundness.

$$roundness = \frac{4 \times area}{\pi \times (Max\ Diameter)^2} \quad (2)$$

Extent: It quantifies how much a shape is stretched through its horizons.

$$extent = \frac{the\ area\ of\ FAZ}{the\ area\ of\ the\ bounding\ rectangle} \quad (3)$$

Convexity: The convex hull is the small-

est convex enclosure that surrounds a shape. For less convex shapes, the value of convexity degrades to zero.

$$convexity = \frac{the\ perimeter\ of\ the\ convex\ hull}{the\ perimeter\ of\ FAZ} \quad (4)$$

Solidity is defined as the ratio of FAZ area over a convex hull.

Table 1 presents the values of these parameters estimated for different synthetic objects. As shown, the parameters can depict the irregularity in the shape. As an example, the more erratic the shape, the more drop, i.e. we can have in the form factor despite the solidity value being contestant.

In addition to the above parameters, we

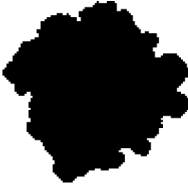
introduced the following two parameters for measuring the contour irregularity of FAZ.

Border Irregularity: The coefficient of variance (CV) of the distance from the centroid for all points on the FAZ boundary is regarded as a border irregularity measure (Figure 7).

$$\text{Border irregularity} = \frac{\sigma_d}{\mu_d} \quad (5)$$

Where σ_d presents the standard deviation of the distance between the boundary points and the centroid; μ_d is the average distance between the boundary points and the centroid.

Table 1: Various parameters calculated for various synthetic shapes.

	Syntetic Shape			
Parameter				
Form Factor	1.01	0.73	0.54	0.55
Roundness	1.00	0.96	0.95	0.92
Extent	0.77	0.67	0.65	0.64
Convexity	1.00	0.89	0.79	0.79
Solidity	0.99	0.93	0.90	0.90
Axial Ratio	1.00	1.02	1.01	1.06
Border Irregularity	0.01	0.06	0.11	0.12
Frequency Irregularity	0.7	8.0	78.5	81.06

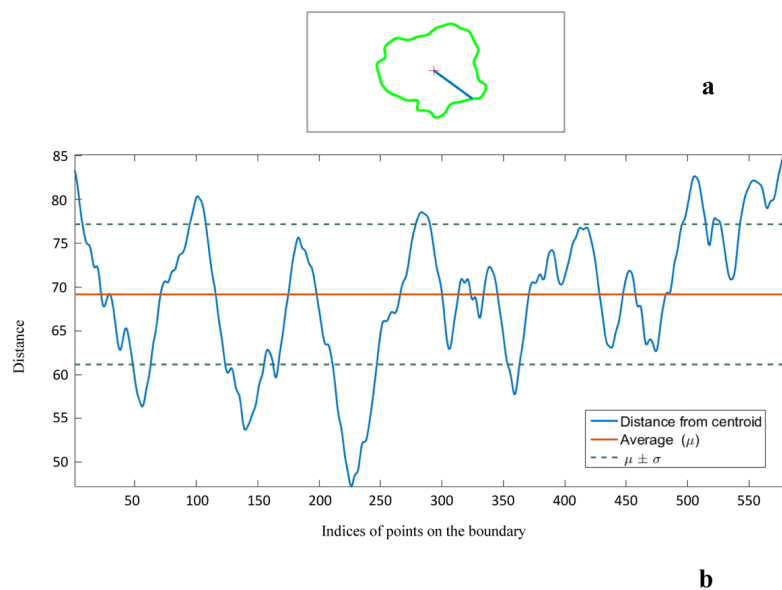


Figure 7: a) A sample boundary of Foveal Avascular Zone (FAZ) with its center. b) The distance of all points on the boundary from the center is shown. Irregularity index is defined as the coefficient of variance of these values.

Frequency domain irregularity: All the points on the boundary were mapped onto the cartesian complex plane as:

$$r_n = x_n + iy_n, n = 0, 1, 2, \dots, N - 1 \quad (6)$$

where (x_n, y_n) represents the coordinates of the n^{th} point on the boundary and N is the number of the points.

Thereafter, the resulting sequence of N complex numbers $\{r_n\}$ was analyzed using discrete Fourier transform (DFT) as:

$$S_k = \mathcal{F}(r) = \sum_{n=0}^{N-1} r(n) e^{-\frac{i 2\pi kn}{N}}, k = 0, 1, 2, \dots, N - 1 \quad (7)$$

In the frequency domain, S_0 corresponds to the coordinates of the centroid (DC component) and S_1 , for instance, represents the largest bounding circle that can be fitted on the boundary. Although S_0 and S_1 do not convey informative features of FAZ shape, for $k > 1$, each S_k highlights a corresponding component that contributes to the irregularity of the boundary. The aggregated frequency-domain energy of these components provides a measure of irregularity which could be considered as a biomarker capable of discriminating groups of subjects.

$$\text{Energy} = \frac{1}{N - 2} \sum_{k=1}^{N-1} S_k S_k^* \quad (8)$$

Evaluation

The effectiveness of the developed software was evaluated using OCTA images from 42 eyes of 21 healthy subjects (11 females and 10 males, age: 42 to 66). The images were acquired by an OCTA instrument (Heidelberg Engineering, Heidelberg, Germany) at Poostchi Eye Research Center, Shiraz, Iran. The size of the images was $3 \times 3 \text{ mm}^2$ with the scale ranging from 5 to 6 $\mu\text{m}/\text{pixel}$. The number of B-scans was 512 with a distance of 6 μm . All images were En face type, with a field of view of $10^\circ \times 10^\circ$ ($\sim 2.9 \times 2.9 \text{ mm}^2$) in high-resolution mode ($\sim 5.7 \mu\text{m}/\text{pixel}$). The scan was conducted for both superficial and deep vascular complex the superficial vascular complex consists of nerve fiber layer vascular plexus and

superficial vascular plexus. The deep vascular complex encompasses intermediate and deep capillary plexus. The protocol of this study was approved by the Research Ethics Committee of the Shiraz University of Medical Sciences and complied with the ethical standards stated in the Declaration of Helsinki. Written Informed consent was obtained from all individual participants included in the study.

The consistency and reliability of the measurements made using the developed software were assessed via repeating the experiment by three independent operators. Interobserver reliability was assessed by intraclass correlation coefficient (ICC) (two-way mixed, absolute agreement, 95% confidence interval) via SPSS 23. The ICC value can be elucidated as poor (< 0.5), moderate ($0.5 \sim 0.75$), good ($0.75 \sim 0.9$), and excellent (> 0.9) [22].

Results

The nine parameters (area, form factor, axial ratio, solidity, roundness, extent, convexity, border, and frequency irregularities) measured using the provided software for the dataset are summarized in Table 2. Results for evaluating the consistency and reliability of the measurements made using the software are provided in Table 3. The ICC value for several measurements such as area, axial ratio, roundness, and extent for both right and left eyes is greater than 0.9 in the superficial layer. Moreover, in the deep layer, the ICC value for area, solidity, roundness, and extent is greater than 0.7 for right and left eyes.

The reliability of the measurement for the two parameters form factor and convexity for the superficial layer are above 0.7 (ICC > 0.7), but for the deep layer are below 0.5 (ICC < 0.5).

Discussion

OCTA imaging provides beneficial information on retinal and choroidal circulations that is useful in evaluating a wide variety of retinal and optic nerve diseases including

Table 2: Summary of the indices measured for Foveal Avascular Zone (FAZ) for 21 healthy subjects using the developed software

Parameter	Superficial Layer	Deep Layer
Area	0.37±0.09 (0.21 to 0.64)	0.32±0.10 (0.12 to 0.51)
Form Factor	0.34±0.05 (0.23 to 0.46)	0.64±0.12 (0.37 to 0.83)
Axial Ratio	1.14±0.07 (1.03 to 1.30)	1.18±0.12 (1.04 to 1.54)
Solidity	0.88±0.03 (0.79 to 0.91)	0.89±0.05 (0.77 to 0.97)
Roundness	0.85±0.07 (0.66 to 0.94)	0.88±0.05 (0.66 to 0.94)
Extent	0.64±0.03 (0.60 to 0.71)	0.66±0.06 (0.56 to 0.81)
Convexity	0.63±0.04 (0.56 to 0.71)	0.85±0.06 (0.73 to 0.93)
Border Irregularity	0.10±0.02 (0.06 to 0.14)	0.12±0.04 (0.06 to 0.29)
Frequency Irregularity	77.39±37.65 (22.9 to 187.4)	87.98±48.56 (20.6 to 251.8)

Table 3: Intraclass correlation coefficient, overall (%95 confidence Interval), for the measurements completed by three independent operators via the software.

Parameter	Eye	Superficial layer	Deep Layer
Area	Right	0.96, (0.86,0.97)	0.73, (0.36,0.89)
	Left	0.96, (0.92,0.98)	0.80, (0.53,0.92)
Form Factor	Right	0.80, (0.59,0.91)	0.46, (0.01,0.75)
	Left	0.60, (0.20,0.82)	0.70, (0.35,0.87)
Axial Ratio	Right	0.96, (0.91,0.98)	0.87, (0.74,0.94)
	Left	0.94, (0.88,0.98)	0.67, (0.33,0.85)
Solidity	Right	0.93, (0.86,0.97)	0.76, (0.50,0.89)
	Left	0.71, (0.39,0.87)	0.85, (0.69,0.93)
Roundness	Right	0.96, (0.91,0.98)	0.87, (0.72,0.94)
	Left	0.90, (0.80,0.96)	0.690, (0.38,0.86)
Extent	Right	0.83, (0.64,0.92)	0.77, (0.52,0.90)
	Left	0.87, (0.74,0.94)	0.83, (0.66,0.93)
Convexity	Right	0.65, (0.27,0.85)	0.41, (-0.04,0.72)
	Left	0.61, (0.20,0.83)	0.52, (0.09,0.78)

AMD, DR, artery and vein occlusions, glaucoma, and multiple sclerosis [3,23].

Previous studies showed promising results of quantitative OCTA for objective evaluation of retinal and optic nerve diseases [5-11]. Particularly, it was revealed that the area of FAZ in the deep and superficial plexus layer is significantly larger for diabetic eyes [11]. However, the reliability of measurements

completed in the quantification of OCTA is vital for the objective evaluation of retinal and optic nerve abnormalities. Nevertheless, manual analyses of OCTA images to calculate metrics related to retinal vascular density and morphology are costly, time-consuming, subject to human error, and are exposed to both inter-and intra- operator variability. Here, we provided details of an interactive software

framework developed for measuring several indices describing microvascular morphology, vessel morphology, and FAZ morphology. The derived indices (Table 2) are consistent with the values reported by Shiihara et al. [17].

In terms of the reliability of the measurements made using the software, as shown in Table 3, the ICC value for several measurements such as area, axial ratio, roundness, and extent for both right and left eyes is >0.9 in the superficial layer, which shows excellent reliability. Moreover, in the deep layer, ICC values for area, solidity, roundness, and extent are above 0.7 for right and left eyes, which are considered good reliable. The reliability of the measurement for the two parameters of form factor and convexity for the superficial layer is good (ICC <0.7), but for the deep layer, it is poor (ICC <0.5). The main reason is that these two parameters are highly dependent on the perimeter of a shape, which depends on the correct detection of the boundary.

The majority of ICC values are higher in the superficial layer in comparison with the deep layer because the vessels are more visible in the superficial layer than in the deep one. Hence, in analyzing the superficial layer, the operator should carefully control or even edit the results of the image processing steps (e.g., FAZ detection); nevertheless, analyzing the superficial layer may not need the interaction of the operator as much as analyzing the deep layer.

Overall, the developed software provides quantitative indices regarding the shape of FAZ and vascular densities in a spreadsheet file that can facilitate further statistical comparison in cohort studies. The indices can be used to develop a decision support system for diagnosing retinal and optic nerve diseases. The software can be used to obtain deeper insights into retinal variations in different populations and to diagnose specific suspected diseases such as diabetic retinopathy (our future work). However, before clinical use, further assessment of the software on a large dataset

is required.

Conclusion

An open-source software framework for quantitative analysis of retinal angiography in optical coherence tomography images is developed using MATLAB. Particularly, the application can be used to measure several indices describing microvascular morphology, vessel morphology, and FAZ morphology including area, perimeter, Feret's diameter circularity, axial ratio, roundness, and solidity. Evaluation using OCTA images from the left and right eyes of 21 healthy subjects showed that the values measured using our software are consistent with those reported by others. The reliability of the measurements assessed using the ICC index showed good consistency between the measurements completed by three operators; however, ICC values for the superficial layer are higher for those of the deep layer.

Acknowledgment

This study was funded by Shiraz University of Medical Sciences (Grant # 96-01-01-15316). The authors wish to thank Mr. Argasi and Dr. Khojasteh the Research Consultation Center (RCC) of Shiraz University of Medical Sciences for their invaluable assistance in editing this manuscript.

Authors' Contribution

M. Afarid and N. Mohsenipoor were responsible to fieldwork management, data collection and analysis. Y. Amirmoezzi, M. Ghofrani-Jahromi, and H. Parsaei designed the study, developed the software, analyzed and interpreted the results. These three authors contributed to drafting the article. All authors revised the manuscript and approved its final version.

Ethical Approval

This study was approved by the Research Ethics Committee of the Shiraz University of Medical Sciences and was in compliance with

the ethical standards stated in the Declaration of Helsinki (Ethic number: IR.SUMS.MED.REC.1397.036).

Funding

This study was funded by Shiraz University of Medical Sciences (Grant # 96-01-01-15316) awarded to H. Parsaei.

Conflict of Interest

None

References

1. Fercher AF, Drexler W, Hitzenberger CK, Lasser T. Optical coherence tomography-principles and applications. *Rep Prog Phys*. 2003;**66**(2):239. doi: 10.1088/0034-4885/66/2/204.
2. Ware HOT, Liu W, Hu J, Zhang H, Sun C. Methodology for Image-driven High-resolution Additive Manufacturing Using Discretized Data Set. *Procedia CIRP*. 2017;**65**:139-44. doi: 10.1016/j.procir.2017.04.008.
3. De Carlo TE, Romano A, Waheed NK, Duker JS. A review of optical coherence tomography angiography (OCTA). *Int J Retina Vitre*. 2015;**1**(1):5. doi: 10.1186/s40942-015-0005-8. PubMed PMID: 27847598. PubMed PMCID: PMC5066513.
4. Matsunaga D, Yi J, Puliafito CA, Kashani AH. OCT angiography in healthy human subjects. *Ophthalmic Surg Lasers Imaging Retina*. 2014;**45**(6):510-5. doi: 10.3928/23258160-20141118-04. PubMed PMID: 25423629.
5. Arend O, Wolf S, Jung F, Bertram B, Pöstgens H, Toonen H, et al. Retinal microcirculation in patients with diabetes mellitus: dynamic and morphological analysis of perifoveal capillary network. *Br J Ophthalmol*. 1991;**75**(9):514-8. doi: 10.1136/bjo.75.9.514. PubMed PMID: 1911651. PubMed PMCID: PMC1042463.
6. Khansari MM, O'Neill W, Lim J, Mahnaz S. Method for quantitative assessment of retinal vessel tortuosity in optical coherence tomography angiography applied to sickle cell retinopathy. *Biomed Opt Express*. 2017;**8**(8):3796-806. doi: 10.1364/BOE.8.003796. PubMed PMID: 28856050. PubMed PMCID: PMC5560841.
7. Jia Y, Bailey ST, Hwang TS, McClintic SM, Gao SS, Pennesi ME, et al. Quantitative optical coherence tomography angiography of vascular abnormalities in the living human eye. *Proc Natl Acad Sci*. 2015;**112**(18):E2395-402. doi: 10.1073/pnas.1500185112. PubMed PMID: 25897021. PubMed PMCID: PMC4426471.
8. Freiberg FJ, Pfau M, Wons J, Wirth MA, Becker MD, Michels S. Optical coherence tomography angiography of the foveal avascular zone in diabetic retinopathy. *Graefes Arch Clin Exp Ophthalmol*. 2016;**254**(6):1051-8. doi: 10.1007/s00417-015-3148-2. PubMed PMID: 26338819. PubMed PMCID: PMC4884570.
9. Gadde SGK, Anegondi N, Bhanushali D, Chidambara L, Yadav NK, Khurana A, et al. Quantification of Vessel Density in Retinal Optical Coherence Tomography Angiography Images Using Local Fractal Dimension. *Investig Ophthalmology Vis Sci*. 2016;**57**(1):246. doi: 10.1167/iovs.15-18287. PubMed PMID: 26803800.
10. Wang Q, Chan S, Yang JY, You B, Wang YX, Jonas JB, et al. Vascular Density in Retina and Choriocapillaris as Measured by Optical Coherence Tomography Angiography. *Am J Ophthalmol*. 2016;**168**:95-109. doi: 10.1016/j.ajo.2016.05.005. PubMed PMID: 27183862.
11. Takase N, Nozaki M, Kato A, Ozeki H, Yoshida M, Ogura Y. Enlargement of foveal avascular zone in diabetic eyes evaluated by en face optical coherence tomography angiography. *Retina*. 2015;**35**(11):2377-83. doi: 10.1097/IAE.0000000000000849. PubMed PMID: 26457396.
12. Kim K, In You J, Park JR, Kim ES, Oh WY, Yu SY. Quantification of retinal microvascular parameters by severity of diabetic retinopathy using wide-field swept-source optical coherence tomography angiography. *Graefes Arch Clin Exp Ophthalmol*. 2021;**259**(8):2103-11. doi: 10.1007/s00417-021-05099-y. PubMed PMID: 33528650.
13. GitHub [Internet]. Mghofrani/OCTA-Quantitative-Analysis: A MATLAB Framework for Quantitative Analysis of Retinal Angiography in Optical Coherence Tomography Images. 2020. Available from: <https://github.com/mghofrani/OCTA-Quantitative-Analysis>.
14. Adhi M, Bonini Filho MA, Louzada RN, Kuehlewein L, Talisa E, Baumal CR, et al. Retinal capillary network and foveal avascular zone in eyes with vein occlusion and fellow eyes analyzed with optical coherence tomography angiography. *Invest Ophthalmol Vis Sci*. 2016;**57**(9):OCT486-94. doi: 10.1167/iovs.15-18907. PubMed PMID: 27442342.
15. Tang FY, Ng DS, Lam A, Luk F, Wong R, Chan C, et al. Determinants of quantitative optical coherence

- tomography angiography metrics in patients with diabetes. *Sci Rep.* 2017;**7**(1):2575. doi: 10.1038/s41598-017-02767-0. PubMed PMID: 28566760. PubMed PMCID: PMC5451475.
16. Gonzalez RC, Woods RE. Digital Image Processing (3rd Edition). USA: Prentice-Hall, Inc; 2006.
 17. Shiihara H, Terasaki H, Sonoda S, Kakiuchi N, Shinohara Y, Tomita M, et al. Objective evaluation of size and shape of superficial foveal avascular zone in normal subjects by optical coherence tomography angiography. *Sci Rep.* 2018;**8**(1):10143. doi: 10.1038/s41598-018-28530-7. PubMed PMID: 29973663. PubMed PMCID: PMC6031610.
 18. Tang W, Guo J, Liu W, Xu G. Quantitative analysis of retinal and choriocapillary vascular density of multiple evanescent white dot syndrome by optical coherence tomography angiography. *Graefes Arch Clin Exp Ophthalmol.* 2020;**258**(8):1697-707. doi: 10.1007/s00417-020-04687-8. PubMed PMID: 32350652.
 19. Lin G, Wang W, Kang C, Wang C. Multispectral MR images segmentation based on fuzzy knowledge and modified seeded region growing. *Magn Reson Imaging.* 2012;**30**(2):230-46. doi: 10.1016/j.mri.2011.09.008. PubMed PMID: 22133286.
 20. Kim AY, Chu Z, Shahidzadeh A, Wang RK, Pulliafito CA, Kashani AH. Quantifying Microvascular Density and Morphology in Diabetic Retinopathy Using Spectral-Domain Optical Coherence Tomography Angiography. *Invest Ophthalmol Vis Sci.* 2016;**57**(9):OCT362-370. doi: 10.1167/iovs.15-18904. PubMed PMID: 27409494. PubMed PMCID: PMC4968771.
 21. Chan TF, Sandberg BY, Vese LA. Active Contours without Edges for Vector-Valued Images. *J Vis Commun Image Represent.* 2000;**11**(2):130-41. doi: 10.1006/jvci.1999.0442.
 22. Koo TK, Li MY. A Guideline of Selecting and Reporting Intraclass Correlation Coefficients for Reliability Research. *J Chiropr Med.* 2016;**15**(2):155-63. doi: 10.1016/j.jcm.2016.02.012. PubMed PMID: 27330520. PubMed PMCID: PMC4913118.
 23. Hagag AM, Gao SS, Jia Y, Huang D. Optical coherence tomography angiography: Technical principles and clinical applications in ophthalmology. *Taiwan J Ophthalmol.* 2017;**7**(3):115-29. doi: 10.4103/tjo.tjo_31_17. PubMed PMID: 28966909. PubMed PMCID: PMC5617355.